International Journal of Innovative Technology and Exploring Engineering (IJITEE)
ISSN: 2278-3075, Volume-8 Issue-5S March, 2019

Optimized Design and Control of a Stand-Alone Hybrid Power System using Modified Cuckoo Search Algorithm

Harish R, Karthick R

Abstract: This paper presents the optimized design and control of a stand-the only hybrid power system with power management function using a modified search algorithm for cuckoo. The hybrid system comprising PV, Wind, Battery and Fuel Cell is connected to a common DC bus from which the load is supplied with a DC-AC converter. The two main sources namely wind and PV are embedded with MPPT controller to obtain optimum output. The battery which supplies the load during reduced PV output and fuel cell with electrolyzer is considered as an additional support of power to the DC bus. In addition, for power management in the hybrid system, the modified cuckoo search algorithm is proposed to improve the DC bus voltage and supervise the power sharing between loads and different sources. The results obtained are compared to the conventional controller to demonstrate the efficiency of the soft computing approach proposed. The whole system is constructed using the MATLAB Simulink environment and the results of the simulation are presented to validate the proposed method.

Index Terms: Hybrid Power system (HPS), Modified Cuckoo search Algorithm, Maximum Power Point Tracking (MPPT), Wind Turbine (WT), Fuel Cell, Electrolyzer.

I. INTRODUCTION

Energy is the prime requirement for the economic development of a country. Since the existence of humanity and till date energy is been extracted from fossil fuels using various technologies. These fuels are super rich but are limited resources which also degrades the environment. Of late many developing nations are still depending on these fossil fuels which make up a large portion of their energy market. Renewable or alternative energy resources are considered a good substitute for these reasons and offer many advantages. The primary advantage is that these sources are renewable and therefore sustainable and environmentally friendly. Solar and wind are the two major resources which is being widely harvested using matured technologies. Meanwhile the major setback of renewable sources is that they are unpredictable and inconsistent [1]-[5]. These drawbacks have motivated the concept of hybrid power system which consists of renewable sources along with conventional sources like diesel generators. Hybrid system utilizes the best features of individual energy source and provides quality power ranging from a few kW to hundreds of kW [6].

These systems deliver a high level of energy security and reliability. Hybrid systems along with storage capabilities are designed to serve the rural electrification and also acts as a backup source for main grid in case of blackout and other contingencies. Therefore prior to design of hybrid power system, an initial survey of load demand and site inspection has to be carried out. These hybrid power systems are classified into two main types of hybrid power systems, which are standalone and connected to the grid.

The primary objective of hybrid power system is to extract maximum energy from the available resources thereby providing quality and reliable power to consumers. Standalone solar and wind energy systems are considered to be the favorite sources because of its availability in abundance at free of cost. A typical hybrid power system consists of the above said standalone systems along with a diesel generator of fuel cell (latest substitute) with energy storage system, a controller unit and power conditioning unit. Different control algorithms are therefore available to extract maximum power from renewable energy sources [7]-[16]. There are numerous MPPT techniques available in literature having different algorithm and hardware components.

Recently fuel cell has replaced the diesel generator in hybrid power system owing to various reasons which includes high generation cost and pollutes environment through greenhouse gases. Fuel cell is a device that directly converts fuel and oxidant chemical energy into electricity. It does not produce any greenhouse gases and also produces output continuously. The operation is battery - like, but a fuel cell is a non - conventional energy source. Fuel cell is characterized by numerous advantages which includes efficiency, fast demand response, fuel flexibility and low cost [17]-[19]. Fuel cells are generally classified depending on the type of electrolyte and their operating temperatures. Among the various fuel cells available, Polymer Electrolyte Membrane Fuel Cell (PEM) type which uses hydrogen as fuel is most preferred because of its high efficiency and low operating temperature.

The advantages of such a hybrid system can be realized only when the sources are sized appropriately and an efficient energy management solution is put in place. A detailed literature survey reveals that there are numerous optimization techniques for energy management problems [19-21]. The management scheme should offer a stable voltage, minimized energy cost and should extract maximum energy available from the source.

Revised Manuscript Received on March 08, 2019.

Harish R, Assistant Professor, Dept. of EEE, SNS College of Engineering, Coimbatore, Tamilnadu, India

Karthick R, Assistant Professor, Dept. of EEE, SNS College of Technology, Coimbatore, Tamilnadu, India

A modified Cuckoo search algorithm for power management is developed in this paper in order to achieve the following objectives.:

- Both PV and wind are operated optimally using suitable MPPT techniques.
- The DC voltage across the bus is maintained constant irrespective to the variations in sources.
- Energy from various sources are managed optimally between loads which ensures reliable quality power to customers.

The paper is organized into the sections below. Section I describes how the paper was introduced. Section II explains the main design of the hybrid power system, which includes solar, wind and fuel cell modelling. The proposed modified Cuckoo search algorithm is also discussed in the same section. Section III discusses the hybrid system simulation model in which the results and discussion are discussed in Section IV. Section V concludes the proposed work.

II. DESIGN AND MODELLING OF HYBRID POWER SYSTEM

The proposed hybrid power system block diagram shown in Figure 1 consists of a solar PV system, a wind turbine system, a fuel cell with an electrolyzer and a battery system. All sources are connected to a convenient electronic interface system to a common DC bus. The energy from solar PV system is harvested through a DC-DC converter which operates in boost mode. As shown in Figure 1, the wind energy system is connected to the DC bus through a back - back connected converter, which includes an uncontrolled AC - DC rectifier unit and a boost converter for DC - DC. The fuel cell is connected by a DC - DC boost converter and the electrolyzer acts as an input to the fuel cell, which also draws power from the DC bus. Finally, the battery system is connected through a bidirectional converter. The detailed modelling of the above sources is discussed in the preceding section.

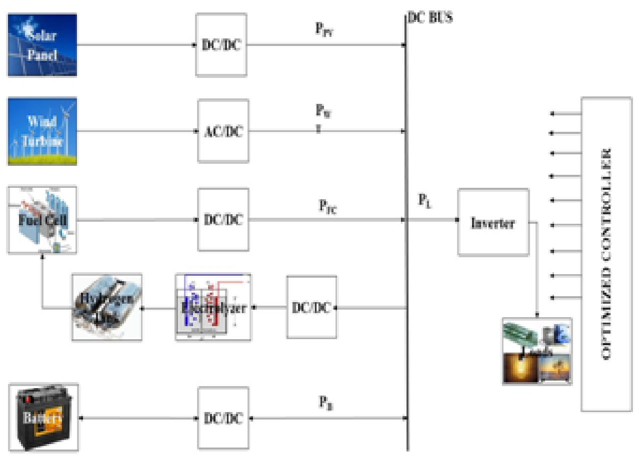

Fig. 1 Block diagram of Hybrid Power Systems

Solar PV system with MPPT Controller

Solar cell is a photovoltaic device that converts sunlight energy into electricity based on photovoltaic effect. The solar energy is interim in nature and depends on various parameters like irradiance and temperature which are natural parameters.

These factors necessitate an accurate model for solar cell that will include the effect of the above factors. Figure 2, from which an expression for the output current is derived [2], shows the equivalent circuit of an ideal solar cell.

$$I = I_L - I_O\left\{exp\left(\frac{V+IR_s}{\eta V_T}\right)-1\right\} - \frac{V+IR_S}{R_{SH}} \quad (1)$$

where, I = output current
I_L = photo generated current
I_D = Diode current
I_{SH} = Shunt current
η = diode ideality factor
V_T= 0.0259 volt

It is seen that the solar cell is modeled in antiparallel to a diode as a current source.

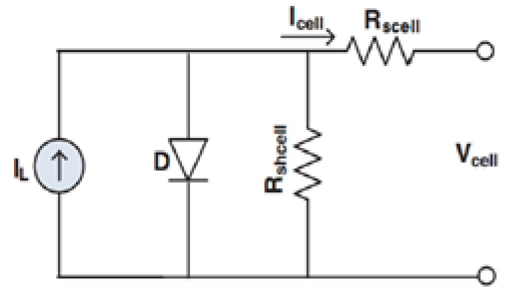

Fig. 2 Equivalent circuit of a PV cell

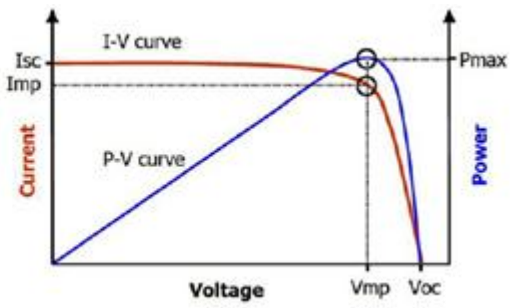

Fig. 3 PV and IV characteristics of PV Cell

The PV module's power characteristics are generally derived from its I-V and P-V characteristics as shown in Figure 3. The figure shows that the power increases to the optimum voltage (i.e. the knee point of the curve) and the power begins to decrease above the optimum point. We also observe from this characteristic that there is a unique point called the Maximum Power Point (MPP), during which the PV panel provides maximum power output. To track this point there are several Maximum Power Point Tracking Algorithm (MPPT) available in literature. In this work, a very powerful and simple algorithm is used to extract maximum power, namely Perturb and Observe (P&O). The algorithm flowchart is displayed in Figure 4.

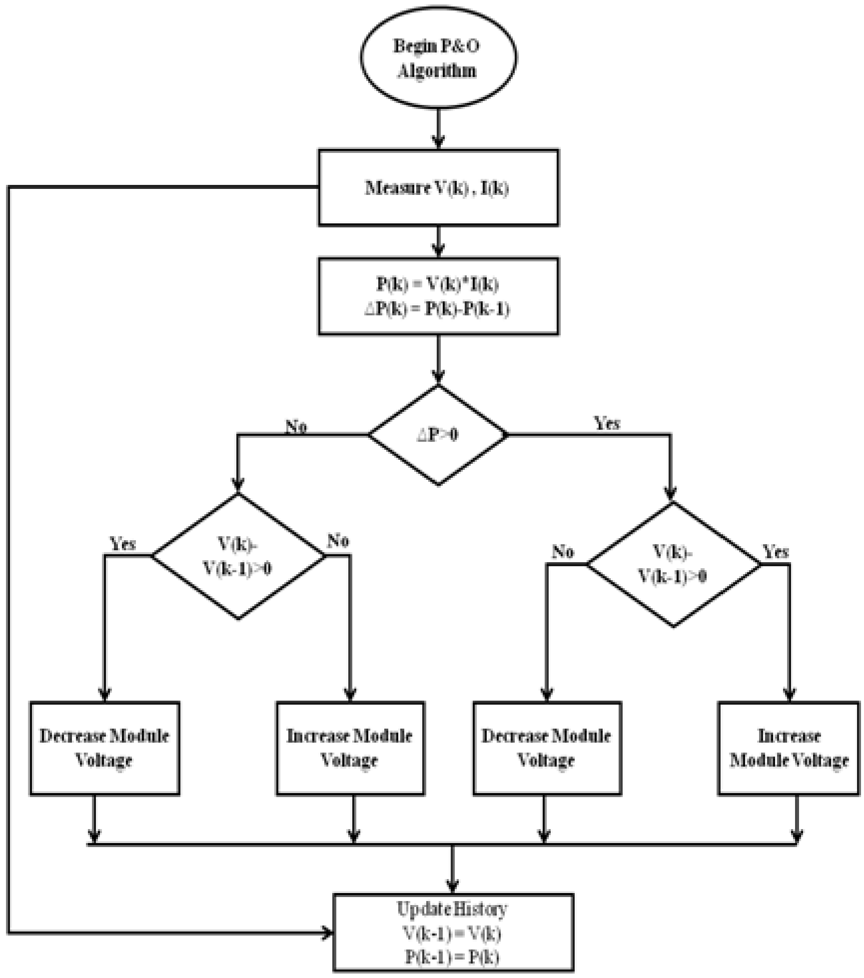

Fig. 4 Perturb and Observe flow chart

Wind Energy Conversion System

The conversion system of wind energy converts kinetic energy into mechanical energy and electrical energy. The system consists of a Permanent Synchronous Magnet Generator (PMSG) and a connected back - to - back converter [2]. The kinetic energy of the flowing air mass per unit time gives the power contained in the wind. That is.

$$P_{air} = \frac{1}{2} \rho A V_{\infty}^{3} \quad (2)$$

where, P_{air} is the power contained in wind (in watts), ρ is the air density (1.225 kg/m^3) at 15°C and normal pressure), A is the swept area in (square meter), and V_∞ is the wind velocity without rotor interference, i.e., ideally at infinite distance from the rotor (in meter per second).

Although Equation (2) provides the wind power, the power transferred to the rotor of the wind turbine is reduced by the power coefficient, C_p

$$C_p = \frac{P_{wind\ turbine}}{P_{air}} \quad (3)$$

$$P_{wind\ turbine} = C_p * P_{air}$$
$$= \frac{1}{2} \rho A V_{\infty}^{3} \quad (4)$$

The Betz limit defines the maximum value of C_p, which states that a turbine can never extract more than 59.3% of the power from an air stream. The tip velocity ratio is set as,

$$\lambda = \frac{\omega R}{V} \quad (5)$$

Where, is rotational rotor speed (in rpm), R is the swept area radius (in meter). The two dimensional parameters, namely the tip velocity ratio λ and the power coefficient C_p, describe the performance of any size of the wind turbine rotor.

The wind turbine output power, i.e. the power supplied by the rotor, is given by:

$$P_t = 0.5\rho$$
$$AC_p(\lambda,\beta) * (v_w)^3 = 0.5\rho AC_p * (\omega_m R/\lambda)^3 \quad (6)$$

where, ρ = air density (kilograms per cubic meter),
v_w = wind speed in meters per second,
A = blades' swept area,
C_p = turbine-rotor-power coefficient, which is a function of the tip-speed ratio (λ) and pitch angle (β).
ω_m = rotational speed of turbine rotor in mechanical radians per second, and
R = radius of the turbine

The coefficient of performance of a wind turbine is influenced by the tip-speed to wind-speed ratio, which is given by

$$TSR = \lambda = (\omega_m R/v_w) \quad (7)$$

The wind turbine can produce maximum power when the turbine operates at maximum C_p (i.e., at $C_{p,opt}$). The rotor speed must therefore be kept at the optimum value of the tip - speed ratio λ_{opt} which is usually achieved using an appropriate MPPT method.

Published By:
Blue Eyes Intelligence Engineering
& Sciences Publication

The DC - DC boost converter's duty ratio is adjusted in this paper to achieve the optimum power output value.

The optimum target power from a wind turbine is given by

$$P_{m\_opt} = 0.5\rho AC_{p\_opt}(\omega_{m\_opt}/\lambda_{opt})^3 = k_{opt}(\omega_{m\_opt})^3 \quad (8)$$

Where $k_{opt} = 0.5\rho AC_{p\_opt}(R/\lambda_{opt})^3$

$$\omega_{m\_opt} = (\lambda_{opt}/R)v_w = k_w * v_w$$

Therefore, the target optimum torque is given by

$$T_{m\_opt} = k_{opt}(\omega_{m\_opt})^2 \quad (9)$$

In view of the fact that the voltage expression of the PMSG in the reference frame of the dq - axes is given under balanced conditions,

$$V_{ds} = R_s i_{ds} + L_d \frac{d}{dt} i_{ds} - \omega_e L_q I_{qs} \quad (10)$$

$$V_{qs} = R_s i_{qs} + L_q \frac{d}{dt} i_{qs} + \omega_e L_d I_{ds} + \omega_e \lambda_r$$

where, V_{ds} and V_{qs} are the instantaneous stator voltages in the dq-axes reference frame, and i_{ds} and i_{qs} are the instantaneous stator currents in the dq-axes reference frame. Here, L_d and L_q are the d-axis and q-axis inductances, and ω_e is the electrical angular speed of the rotor, while λ_r is the maximum phase flux linkage due to the rotor.

Fuel Cell

A fuel cell is a device that directly converts the fuel and oxidant's chemical energy into electricity [2]. The fuel cell operation is determined by the following equation.

$$Anode: H_2 \rightarrow 2H^+ + 2e$$

$$Cathode: \frac{1}{2}O_2 + 2H^+ + 2e^- \rightarrow H_2O$$

$$Overall: H_2 + \frac{1}{2}O_2 \rightarrow H_2O + \text{electrical energy} + \text{heat} \quad (11)$$

The dynamic modeling of fuel cell is given by,

$$V_{fc} = E_{cell} - V_{act} - V_{con} - V_{ohmic} \quad (12)$$

where, E_{cell} = The cell's thermodynamic potential.

V_{act} = activation overvoltage

V_{ohmic} = ohmic overvoltage.

V_{con} = concentration overvoltage

The Nernst equation based on above expression is given by,

$$E_{cell} = E_{0,cell} + \frac{RT}{2F}\left[lnP_{H2} + \frac{1}{2}lnP_{O2}\right] \quad (13)$$

Where, T is the temperature of the cell (K), P_{H2} is the partial pressure of hydrogen and P_{O2} is the partial pressure of oxygen at the anode and cathode, and $E_{0,cell}$ is the voltage of the open circuit:

$$E_{0,cell} = E^0_{0,cell} - k_E(T - 228) \quad (14)$$

The Overvoltage of activation (loss due to anode and cathode activation) in a fuel cell provided by,

$$V_{act} = -[\zeta_1 + \zeta_2 T + \zeta_3 T ln(C_{o2}) + \zeta_4 T ln(i_{FC})] \quad (15)$$

Co2 is the concentration of dissolved oxygen at the liquid gas interface, where i_{Fc} is the operating current of the cell and ζ_1, ζ_2, ζ_3, ζ_4 is the parametric coefficient of the fuel cell.

Ohmic loss of fuel cell is expressed as,

$$V_{ohmic} = i_{FC}(R_{el} + R_{pr}) \quad (16)$$

Where, R_{el} is the electron flow membrane resistance and R_{Pr} is the proton flow resistance.

The concentration voltage drop due to reaction process is given by,

$$V_{con} = -B * ln\left[1 - \frac{j}{j_{max}}\right] \quad (17)$$

Where B represents a parametric coefficient (v) and j represents the cell's actual current density (A/cm2) and j_{max} is the limiting current density.

Assuming the lumped parameter representation of fuel cell stack, the total output voltage is given by,

$$v_{out} = N_{cell} * V_{cell} = N_{cell}(E_{cell} - V_{act} - v_{ohmic} - v_{con}) \quad (18)$$

Where, N_{cell} = Number of stacked fuel cell.

V_{cell} = fuel cell voltage.

E_{cell} = The fuel cell's thermodynamic potential.

V_{act}, v_{con}, v_{ohmic} are losses introduced into the fuel cell.

Electrolyzer

An electrolyzer is an electrochemical device which splits water into hydrogen and oxygen using electric current. According to Faraday's law, the amount of hydrogen produced in an electrolyzer cell is directly proportional to the total number of electrons emitted from the electrodes, which is nothing other than the equivalent electrical current in the circuit [2]:

$$n_{H_2} = \frac{\eta_F \cdot \eta_n \cdot i_e}{2F} \quad (19)$$

$$\eta_F = 96.5 \times \left[e^{\frac{0.09}{i_e} - \frac{75.5}{i_e^2}}\right]$$

η_{H_2} = Hydrogen production rate, mol s^{-1},

η_F = Faraday's efficiency,

n_c = the number of electrolyzer cells in series

i_e = electrolyzer current [A]

F = Faraday constant [C kmol-1]

III. OPTIMIZED ENERGY MANAGEMENT SYSTEM

Since the renewable energy sources are unpredictable and interim in nature, there is always a possibility of power imbalance when the load is connected. Hence a coordinated supervisory control is required to overcome the power imbalance in the system. In this paper, an optimized energy management based on Cuckoo Search Algorithm is proposed to coordinate all sources and load. The CS algorithm will always search for the optimum combination which entirely rely on random walk that does not rely on faster convergence. In this proposed method, two modifications are done to increase the convergence rate thereby making the algorithm more suitable for practical applications. The various possible operating modes are summarized in table.1

Table. 1 Operating Conditions

MODE	OPERATING CONDITIONS
Mode 1	• The output power from solar and wind is equal to the load demand ($P_{solar} + P_{wind} = P_L$) Power = 3500 Watts
Mode 2	• The output power from solar and wind is less than the load demand ($P_{solar} + P_{wind} < P_L$) Power = 2500 Watts • The battery will supply power to the load • Until the SOC of the battery becomes to 20%
Mode 3	• The case of high-power source ($P_{net} > 0$),the excess energy is supplied into the electrolyzer to generate hydrogen power = 3700 Watts • The control is carried out by comparing the SOC limit of battery.
Mode 4	• The case of inability of the sources to ensure the load demand ($P_{net} < 0$), • The fuel cell produce energy for Load. Power = 3500 Watts • Until the SOC of the battery becomes to 80%

The flowchart for the proposed optimized energy management system is shown in figure 5. The process gives prime importance to the main sources like solar and wind. Both the major sources are always operated at their maximum power point using their MPPT.

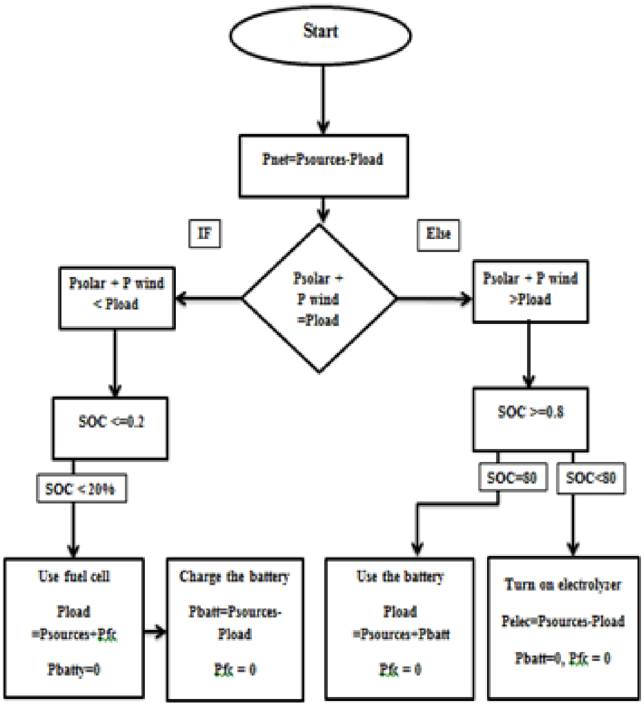

Fig. 5 Flowchart for Optimized Energy Management System

IV. SIMULATION RESULTS

MATLAB / Simulink software models and simulates the complete hybrid model with all sources and loads. The parameters used for various models are presented in Appendix-I. MATLAB has A 2 Kw solar panel. As shown in Figure 6, the PV array was interfaced with the boost converter.

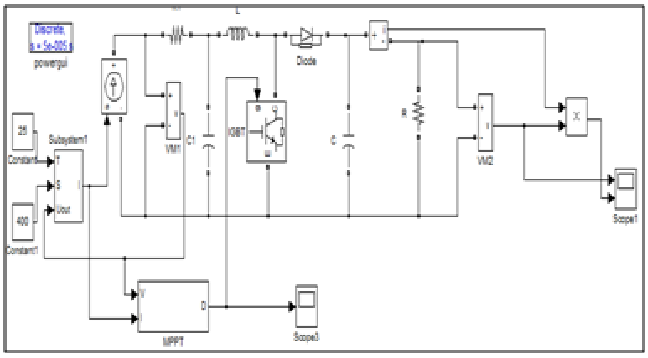

Fig. 6 Simulink model of PV system with boost converter

The figure 7 describes wind energy conversion model consisting of PMSG with uncontrolled rectifier of 1.5 Kw and the boost converter.

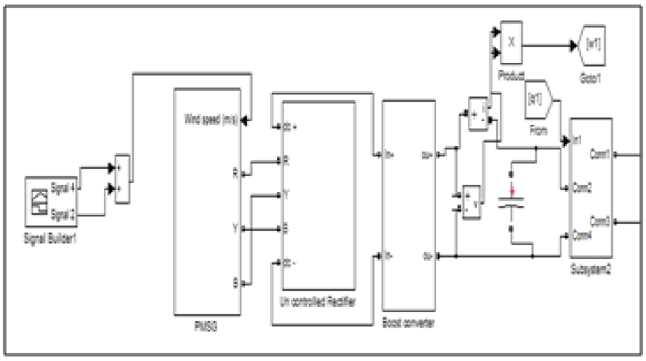

Fig. 7 Simulink model of WECS with back to back converter

Simulation Results of Hybrid System without MCSA

The simulation results for the proposed system is realized from the system without utilizing any control technique and their respective outputs are shown in below figures 8 (a) – 8 (c).

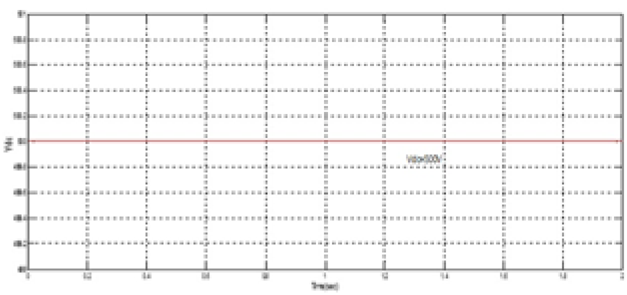

Fig. 8 (a) DC Link Voltage With-Out MCSA

Published By:
Blue Eyes Intelligence Engineering
& Sciences Publication

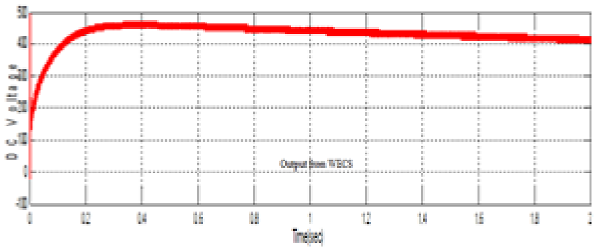

Fig. 8 (b) DC Voltage of PMSG with Boost Converter

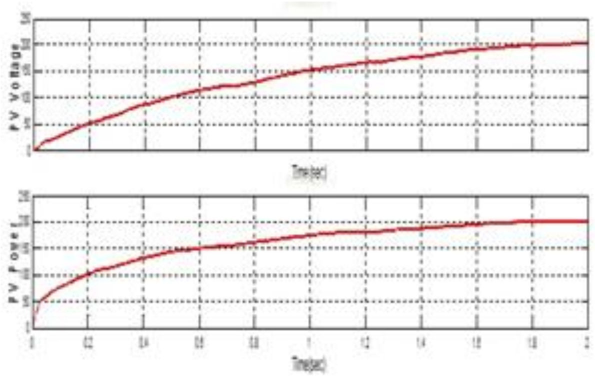

Fig. 8 (c) Output of PV Voltage and PV Power

Figure 8 (a) shows the voltage of the DC connection and it is shown that the voltage is not constant as the reference voltage indicates. The change PV voltage and power are shown in figure 8 (b). It is observed that without any controller the output varies with respect to irradiance and temperature. Figure 8 (c) shows the output from wind energy conversion system after being rectified and here also it is observed that the DC output is changing when the wind speed varies.

Simulation Results of Hybrid System with MCSA

Mode – 1 Operation

The DC connection voltage is kept constant at 600Vdc in this mode of operation, as shown in Figure 9 (a). Figure 9 (b) shows the DC voltage of the WECS output, which is a constant output with MPPT technology. Figure 9 (c) shows the PV output DC voltage and the single phase 230V DC. The output power of 3500W is shown in Figure 9 (e).

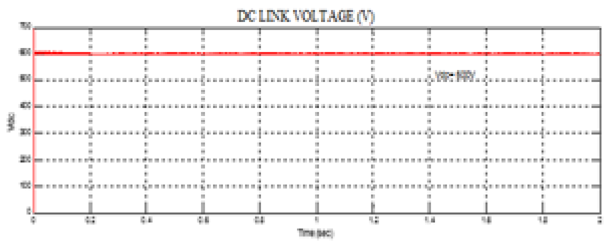

Fig. 9 (a) DC Link Voltage for Mode-1 Operation

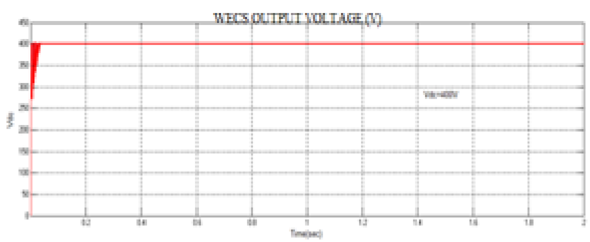

Fig. 9 (b) WECS Output DC Voltage

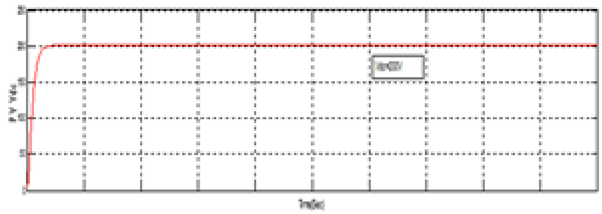

Fig. 9 (c) PV Output Voltage during mode 1 operation

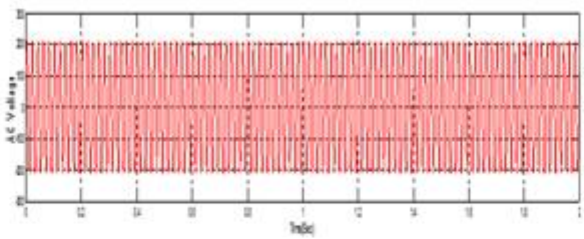

Fig. 9 (d) Single Phase AC 230 V output voltage

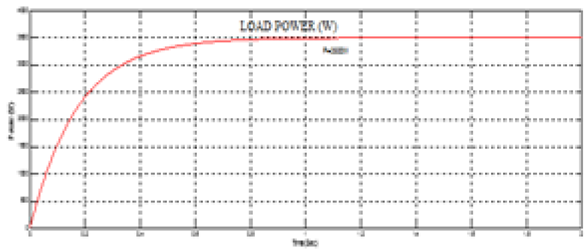

Fig. 9 (e) Output of the Load Power-mode 1 operation

Mode – 2 Operation

Due to the increase in load to 500 Vdc as shown in Figure 10 (a), the DC connection voltage is reduced in mode-2. Figure 10 (b) shows that the WECS constant DC voltage and PV is reduced to 100Vdc as shown in Figure 10 (c), the load output power is reduced to 1900W as shown in Figure 10 (e).

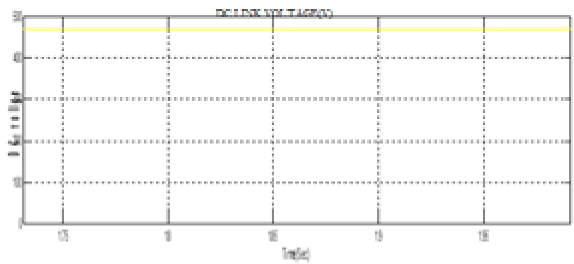

Fig. 10 (a) DC Link Voltage for Mode-2 Operation

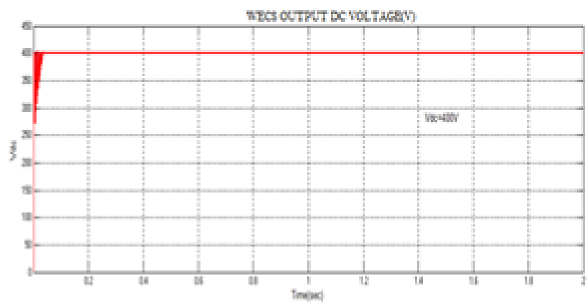

Fig. 10 (b) WECS Output DC Voltage

Published By:
Blue Eyes Intelligence Engineering
& Sciences Publication

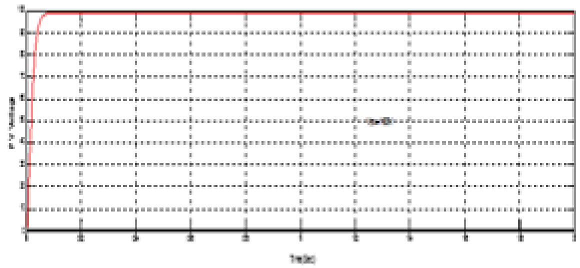

Fig. 10 (c) PV Output Voltage-mode II operation

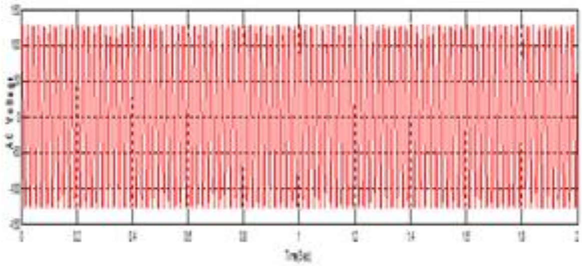

Fig. 10 (d) Single Phase AC 130 V output voltage

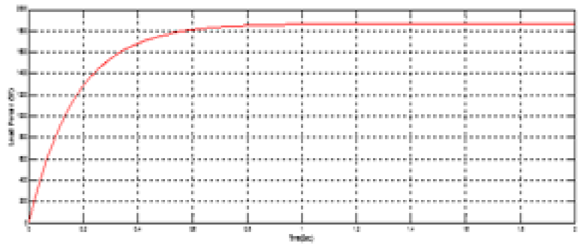

Fig. 10 (e) Output of the Load Power- mode 1 operation

Mode – 3 Operation

The DC connection voltage in this mode is 620V dc as shown in the figure. Figure 11(b) - 11(d) shows the wind, PV and battery voltage in the DC mode - 3 operation in which the voltage of the DC connection is reduced and the remaining voltage is injected by the battery to compensate. Figure 11 (e) shows the percentage of battery discharge by charging state as shown. The output power is displayed in the 4500W figure 11 (g).

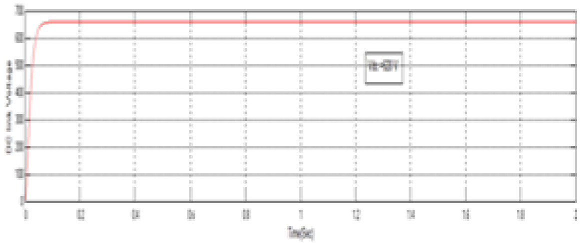

Fig. 11 (a) DC Link Voltage for Mode-3 Operation

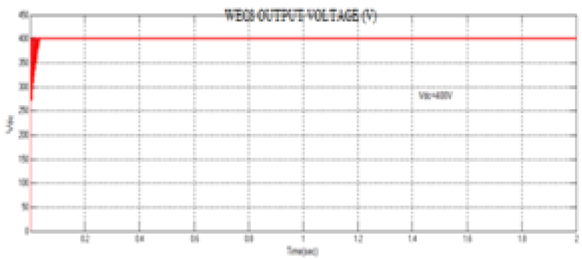

Fig. 11 (b) WECS Output DC Voltage-mode 3 operation

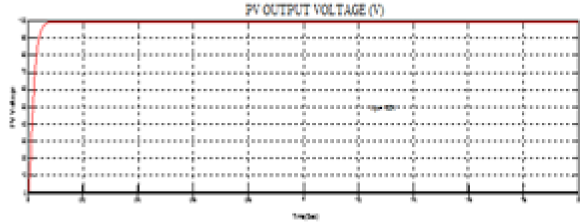

Fig. 11 (c) PV Output Voltage – mode 3 operation

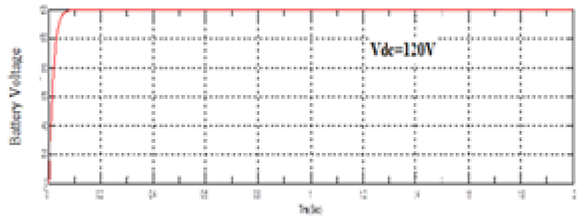

Fig. 11 (d) Battery Output DC Voltage-mode 3 operation

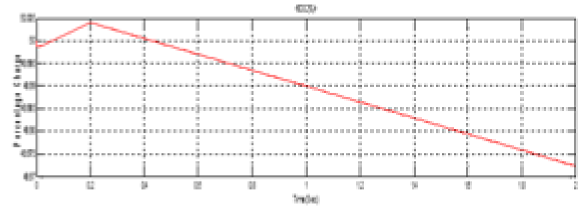

Fig. 11 (e) Battery State of Charge Discharging Percentage – mode 3 operation

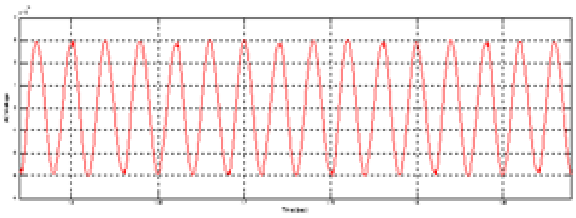

Fig. 11 (f) Single Phase AC 300 V – mode 3 operation

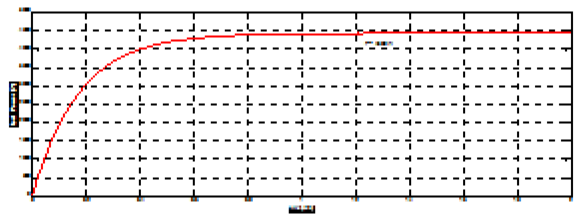

Fig. 11 (g) Output of the Load Power – mode 3 operation

Mode - 4 Operation

The DC connection voltage is shown in Figure 12 (a), and the wind DC voltage is shown in Figure 12 (b). In the battery, state of charge is given in percentage were 20% to 80 % shown in figure 12 (c), here the electrolyzer is been charged to inject hydrogen to the fuel cell and the DC output voltage as shown in figure 12 (d). The given figure 12 (e) shows the battery charging voltage and the percentage of state of charge till it reaches 80 %. Thus, the fuel cell's output power is shown in figure 12 (g), and the total power is shown in figure 12 (h).

Published By:
Blue Eyes Intelligence Engineering
& Sciences Publication

So, here the modes of operation show the power management of the system with modified cuckoo search algorithm is done and validated by the output waveforms of voltage and power.

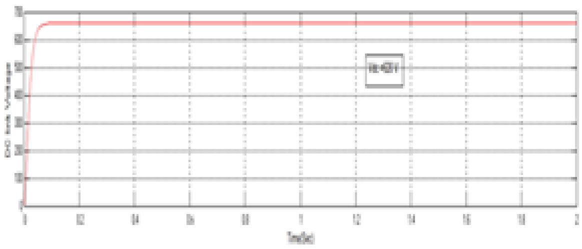

Fig. 12 (a) DC Link Voltage for Mode-4 Operation

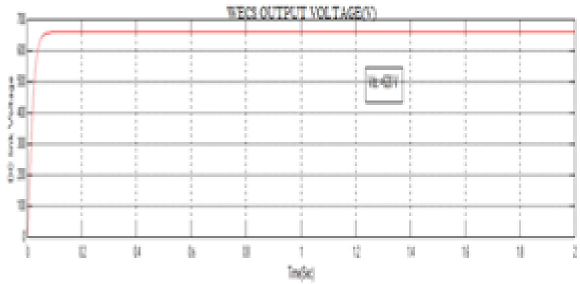

Fig. 12 (b) WECS Output DC Voltage – mode 4 operation

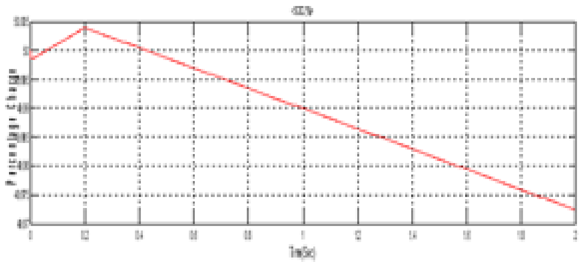

Fig. 12 (c) Battery State of Charge Discharging Percentage

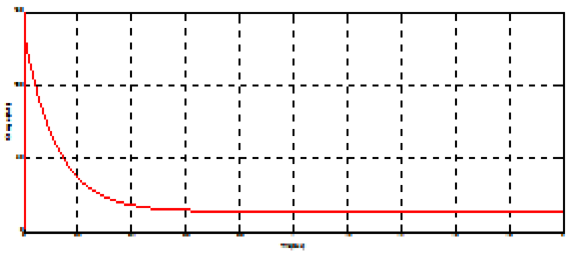

Fig. 12 (d) Electrolyzer Charge Percentage

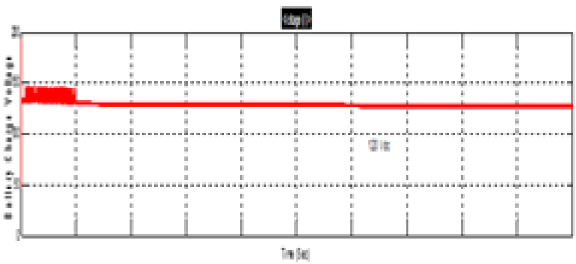

Fig. 12 (e) Battery charge voltage – mode 4 operation

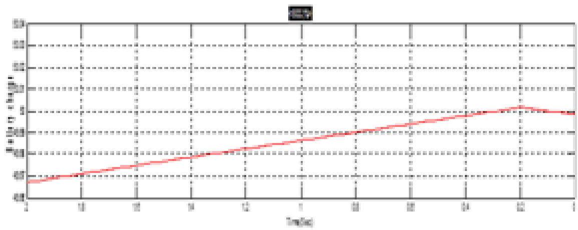

Fig. 12 (f) State of Charging of Battery – mode 4 operation

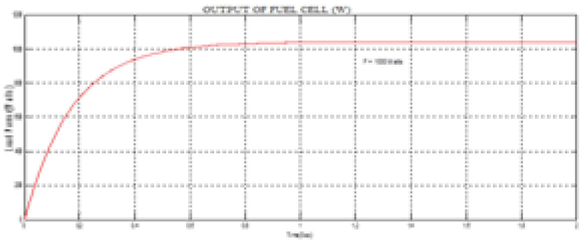

Fig. 12(g) Output Power of Fuel Cell- mode 4 operation

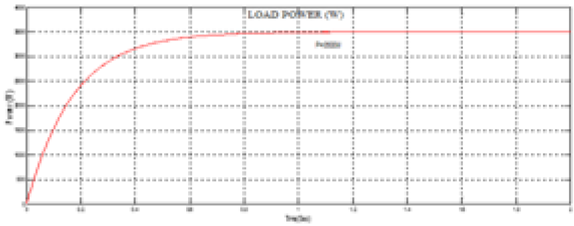

Fig. 12 (h) Total Output Load Power - mode 4 operation

V. CONCLUSION

This paper proposes an optimized energy management system using Cuckoo-Search algorithm for the hybrid power system comprising solar PV, wind, fuel cell and battery. The validity of the proposed system is tested under different operational and environmental conditions. The voltage across the DC bus is verified with and without a controller. The simulation results show that the DC bus voltage is kept at a constant value regardless of the different load conditions and the controller also ensures maximum power from both primary sources such as solar and wind. Finally, the optimized intelligent controller achieves a coordinated control among various power sources and load besides providing a continuous power supply with high reliability. The simulation results show that the intelligent controller works in both stable and dynamic conditions satisfactorily.

Appendix-I Parameters of the System

Permanent Magnet Synchronous Generator	
Nominal power (P_n)	1.5 Kw
Phase inductance of the stator (L_s)	8.4 mH
Phase resistance of the stator (R_s)	0.425 Ω
Number of poles pairs (P)	10
Air density (ρ)	1.225 Kg m^{-3}
Solar Panel	

Published By:
Blue Eyes Intelligence Engineering
& Sciences Publication

Open circuit voltage (V)	32.9 V
Short circuit current (A)	8.21 A
Temperature (°C)	25
Irradiance (W/m^2)	≥900
Number of series cells (N_s)	54
Maximum Power (Pmax)	200 W
Fuel Cell	
Exchange current (Io)	6.54 mA
Current internal (In)	230 mA
Activation voltage constant (A)	1.35V
Mass transfer constant (B)	1.29 V
FC internal Resistance (R_{int})	0.045Ω
No of fuel cell connected in series (N_s)	10
No of fuel cell connected in parallel (N_p)	1
Electrolyzer	
Faraday's constant (F)	96,484,600 cKmol
Number of electrolyzer cells(η_c)	20
Battery	
Rated voltage (V)	200
Rated current (A)	15
Rated capacity (Ah)	150

Appendix-II Modified Cuckoo Search Algorithm

A← Maxlevy Step size
φ←Golden ratio
Initialise a population of n nest x_i (i=1,2,…n)
For all x_i do
Calculate fitness f_i=f(x_i)
End for
Generation number G ←1
While Number of objectives Evaluations
< MaxNumber Evaluations do
G←G+1
Sort nest by order of fitness
For all nests to be abandoned do
Current Position x_i
Calculate Levy flight step size α←A⁄√G
Perform Levy flight from x_i to generate new egg x_K
x_i←x_K
F_i←f(x_i)
End for
For all of the top nests do
Current Position x_i
Pick another nest form the top nest at random x_j
If x_i=x_j then
Calculate Levy flight step size α←A⁄G^2
Perform Levy flight from x_i to generate new egg x_K
F_k=f(x_k)
Choose a random nest l from all nests
If (F_K>F_j) do
x_l←x_K
F_l←F_K
End if
Else
dx=|x_i-x_j |/φ
Move distance dx from the worst nest to the best nest to find x_K
F_K=f(x_K)
Choose a random nest l from all nests
If (F_K>F_l) then
x_l←x_K
F_l←F_k
End if
End if
End for
End while

REFERENCES

1. Bouthaina Madaci , Rachid Chenni , Erol Kurt , Kamel Eddine Hemsas , "Design And Control of a Stand-alone Hybrid Power System," International Journal of Hydrogen Energy, vol.41, No.29, pp.12485-12496, 2016.
2. R.Karthick, S.Manoharan. "Fuzzy based optimised energy management strategy of renewable energy sources for stand – alone applications", Journal of Electrical Engineering, Vol.17, No.1, pp.418-426, 2017.
3. Valenciaga F, Evangelista CA., "Control design for an autonomous wind-based hydrogen production system", Int Journal of Hydrogen Energy, vol.35, no.11, pp.5799-5807, 2010
4. Malla SG, Bhende CN. "Voltage control of stand-alone wind and solar energy system", Int J Electr Power Energy Systems, Vol.56, pp.361-393, 2014.
5. M. H. Nehrir, C. Wang, K. Strunz, H. Aki, R. Ramakumar, J. Bing, Z. Miao, and Z. Salameh.: A Review of Hybrid Renewable/Alternative Energy Systems for Electric Power Generation: Configurations, Control, and Applications. In: IEEE transactions on sustainable energy, vol. 2(2011), no. 4, October 2011, p.392-403.
6. T. Logeswaran,A. Senthilkumar, P. Karuppusamy, "Adaptive Neuro-Fuzzy Model for Grid-Connected Photovoltaic System," International Journal of Fuzzy Systems, Vol.17, No.4, pp.585-594, 2015.
7. Villavla MG, Gazoli JR, Filho ER. "Comprehensive approach to modeling and simulation of photovoltaic arrays". IEEE Tran Power Electron, vol.24, no.5, pp.1198-1208, 2009.
8. S. Ozdemir, N. Altin, I. Sefa, G. Bal "PV Supplied Single Stage MPPT Inverter for Induction Motor Actuated Ventilation Systems," Elektronika ir elektrotechnika, vol. 20, no. 5, pp.1392-1215, 2014.
9. Arteaga Orozco MI, V_azquez JR, Salmer_on P, P_erez A., "A sliding maximum power point tracker for a photovoltaic system", 11th Spanish Portuguese Congress on Electrical Engineering, July 2009.
10. Y. Uzun, S. Demirbas, E. Kurt, "Implementation of a New Contactless Piezoelectric Wind Energy Harvester to a Wireless Weather Station", Elektronika ir elektrotechnika, vol. 20, no. 10, pp.1392-1215, 2014.
11. Datta A, Bhattacharya G, Mukherjee D, Saha H, "An efficient technique for controlling power flow in a single stage grid connected photovoltaic system", International Journal of Science and Technology, vol.21, no.3, pp.885-897, 2014.
12. Bendib B, Krim F, Belmili H, Almi MF, Boulouma S. Advanced fuzzy MPPT controller for a stand-alone PV system, Energy Procedia, Vol.50, pp.383-392, 2014.
13. Zainuri MAAM, Radzi MAM, Soh AC, Rahim NA, "Development of adaptive perturb and observe-fuzzy control maximum power point tracking for photovoltaic boost dc-dc converter", IET Renew Power Generation, Vol.8, No.2, pp.183-194, 2014.
14. Hiroshi N, Tatsuya N, Hiroshi M, Takenobu K. "Development of 100-W high-efficiency MPPT power conditioner and evaluation of TEG system with battery load. Journal of Electronic Materials, vol.40, no.5, pp.657-661, 2011.
15. Nordin AHM, Omar AM., "Modeling and simulation of photovoltaic (PV) array and maximum power point tracker (MPPT) for grid-connected PV system". In: 3rd Int. Symp. Exhibition in Sustainable Energy & Environment, Melaka, Malaysia, June 2011.

16. Ishita Biswas, Vaishalee Dash, Prabodh Bajpai, “Sizing Optimization of PV-FC-Battery System with Hybrid PSO-EO Algorithm”, Annual IEEE India Conference, 2012.
17. Yun Wanga, Ken S.Chen Jeffrey Mishler, Sung Chan Cho, Xavier Cordobes Adroher, “A Review of Polymer Electrolyte Membrane Fuel Cells Technology, Applications and needs on Fundamental Research. In: Applied Energy, vol. 88, no.4, pp.981–1007, 2011.
18. Khazaee I, Ghazikhani M, Mohammadiunc M. “Experimental and thermodynamic investigation of a triangular channel geometry PEM fuel cell at different operating conditions”, Scientia Iranica, vol.19, no.3, pp.585-593, 2012.
19. Rong-Jong Wai, Shih-Jie Jhung, Jun-Jie Liaw and Yung- Ruei Chan.: Intelligent Optimal Energy Management System for Hybrid Power Sources Including Fuel Cell and Battery. In: IEEE transactions on power electronics, vol.28(2013), no. 7, July 2013, p.3231-3244.
20. Erkan Dursun and Osman Kilic, “Comparative evaluation of different power management strategies of a stand-alone PV/ Wind / PEMFC hybrid power system”, Electrical Power and Energy Systems, Vol. 34, No.1, pp. 81-89, 2012.
21. Dimitris Ipsakisa, Spyros Voutetakisa, Panos Seferlisa, Fotis Stergiopoulosa and Costas Elmasidesb, “Power management strategies for a stand-alone power system using renewable energy sources and hydrogen storage”, International Journal of Hydrogen Energy, Vol. 34, No.16, pp. 7081-7095, 2009.